Hindawi
Shock and Vibration
Volume 2020, Article ID 8872438, 11 pages
https://doi.org/10.1155/2020/8872438

Research Article

Experimental Investigation on the Influence of Water Content on the Mechanical Properties of Coal under Conventional Triaxial Compression

Meichang Zhang[1] **and Rongshan Nie**[2]

[1]*Liaoning Technical University, Fuxin 123000, Liaoning, China*
[2]*State Key Laboratory of Coal Mine Safety Technology, China Coal Technology & Engineering Group Shenyang Research Institute, Fushun 113122, China*

Correspondence should be addressed to Meichang Zhang; 471610048@stu.lntu.edu.cn

Received 23 May 2020; Revised 28 June 2020; Accepted 11 July 2020; Published 27 July 2020

Academic Editor: Xuesheng Liu

The presence of water is one of the most important factors in coal mining, and it has a dual influence on the mechanical behavior of rock. To study the influence of water content on the mechanical properties of coal under complicated stress conditions, dry coal specimens and wet coal specimens with water contents of 1.8% and 3.6% were conducted by uniaxial and conventional triaxial compression tests. The relations between the uniaxial compressive strength, deformation, and water content were observed. The reductions in the strength and elastic modulus under different confining pressures were obtained. The mechanical properties of coal specimens with different water contents under triaxial compression were studied. The influences of water content on the microstructure, clay minerals, internal friction angle, and cohesive force of coal were discussed. The results show that the strengths and elastic moduli of wet specimens are clearly lower than those of dry specimens under different confining pressures. The water content has a significant influence on the postfailure mechanical behavior of coal. The loss rates of strength and elastic modulus decrease with increasing confining pressure. The water content has almost no effect on the internal friction angle, while the cohesive force of the saturated specimens is 36.5% lower than that of the dry specimens. The results can provide a reference for inhibiting the occurrence of disasters during coal mining and exploiting coal efficiently.

1. Introduction

Water is one of the most important factors in rock engineering. On one hand, water injection is an effective method for mitigating and preventing rockburst [1–3], coal bumps [4], and coal and gas outburst disasters [5]. On the other hand, water can change the microstructure of rock [6–8], induce stress redistribution around a tunnel, and lead to damage or failure of the rock due to a change in its mechanical properties [9]. For example, heavy rains in the summer months may result in landslides [10], water bursting in mines [11], roof fall, and pillar instability [12]. The seepage of water around a reservoir can induce the sliding of surface faults [13], resulting in the occurrence of earthquakes. Therefore, it is necessary to study the influence of water content on the mechanical properties of rock materials to prevent disasters and evaluate the stability of rock engineering.

Many scholars have revealed that water content has a significant influence on rock strength [14], elastic modulus [15], ultrasonic wave velocity [7], and creep behavior [16]. For example, Vásárhelyi [17] found that the uniaxial compressive strength and elastic modulus of saturated limestone are 34% lower than those of the corresponding dry specimens. Dyke and Dobereiner [18] considered that the presence of a small amount of water can lead to large changes in the strength and deformation of rock. Hawkins and Mcconnell [19] found that the presence of water has a significant effect on the mechanical properties of quartz and clay minerals. Hashiba and Fukui [20] determined that the

ratio of the reduction rate under uniaxial tension to that under uniaxial compression was approximately 1.61. Zhou et al. [21] found that the average static compressive strength and tensile strength of saturated sandstones were reduced by 29.9% and 66.5%, respectively, compared to the results for the corresponding dry specimens. Fan et al. [22] considered that water can mitigate the burst tendency of igneous rock, although the current support system needs to be reconsidered. The above studies provide a better understanding of the mechanical properties of saturated rocks.

Coal is a special rock in for energy development, and its need has reached a new level. Currently, mining can extend deeper [23–25], but the coal mining-induced stress state is complex [26–28], which results in the frequent occurrence of dynamic disasters. To this end, many hydraulic measures, such as water injection and hydraulic flushing, were used to mitigate the burst tendency of coal. Therefore, the influence of water content on the mechanical properties of coal under complex stress conditions cannot be ignored. Wang et al. [29] found that the strengths of coal specimens saturated for seven days are 52% lower than those of natural coal specimens. Gu et al. [30] proposed a constitutive model considering the damage by water to describe the deformation of coal. Yao et al. [31] investigated the effect of different soaking times and incident energy magnitudes on the dynamic behavior of coal, considering that it has an optimum water content to resist dynamic loading. Liu et al. [32] studied the directional permeability evolution of intact and fractured coal subjected to true triaxial stress under dry and water-saturated conditions, and it was found that the water content is important for reducing the permeability by up to one order of magnitude. However, there are few experimental studies on the influence of different water contents on the mechanical properties of coal under triaxial compression. Due to complicated geological conditions [33, 34], the study of the mechanical behaviors of coal masses with different water contents has become very practical and meaningful.

The aim of this work is to study the influence of water content on the mechanical properties of coal under complicated stress conditions. To this end, dry coal specimens and wet coal specimens with water contents of 1.8% and 3.6% are subjected to uniaxial and conventional triaxial compression tests. The effect of water content on the strength, deformation, and failure pattern of three groups of specimens was investigated. The results can provide a reference for inhibiting the occurrence of disasters during coal mining and exploiting coal efficiently.

2. Experimental Methods and Preparation

2.1. Coal Sample Preparation. The coal samples were taken from the Hanjiawa No. 22 coal mine in Shanxi Province, China. The inclination angle of the coal seam is approximately 2–6°; it is a subhorizontal coal seam. The thickness of the coal seam is 7.14–11.61 m, and it is a stable, thick coal seam. This coal is long-flame coal. The conventional industrial analysis parameters of the coal samples are listed in Table 1. The chemical components of the coal are mainly made up of SiO_2 (46.05%), AI_2O_3 (39.15%), Fe_2O_3 (6.09%), CaO (3.29%), SO_3 (2.01%), and TiO (2.34%). The tensile strength is 1.91 MPa, and the P-wave velocity ranges from 2076 m/s to 2265 m/s. Cylindrical specimens with a diameter of 50 mm and a height of 100 mm were drilled from an intact coal block, as shown in Figure 1. According to the suggestions by the International Society of Rock Mechanics (ISRM) [35], the specimens were processed with a surface roughness of less than 0.02 mm, and the perpendicularity of the end surface was less than 0.001 rad.

All the specimens remained naturally dry indoors for 7 days, after which time the specimens were considered to have reached a dry state. After that, three dry specimens were put into a water container for different soaking times to reach different water contents at ambient temperature. To obtain the different water contents, the soaking times were set to 4, 8, 14, 24, 48, 72, 96, and 120 h. After every water immersion, the weight of the specimen was recorded by using an electronic balance with an accuracy of 0.1 g, and then the specimen was put back into the water container immediately to conduct the next tested soaking time. According to the weight increase at different soaking times, the water content can be determined:

$$w = \frac{(m_t - m_d)}{m_d} \times 100\%, \quad (1)$$

where w (%) is the water content of the specimen and m_t and m_d are the weights of the wet and dry specimen for a certain soaking time, respectively.

The variation in the water content with increasing soaking time is shown in Figure 2. It can be seen that the water content presents a rapid increase before the soaking time of 24 h. Then, the increase rate of the water content becomes slow. After the soaking time of 48 h, the water content exhibits no significant change, indicating that the coal specimen is in a saturation condition. This phenomenon is in good agreement with the results of previous studies on rock and coal specimens [6, 21, 31]. As shown in Figure 2, the water content of this coal under saturation conditions is approximately 3.6%.

In this paper, three representative water contents were selected to study the effect of water on the mechanical properties of coal specimens: 0%, 1.8%, and 3.6%. The corresponding soaking times are 0, 4, and 120 h, respectively. All the specimens were divided into three groups labeled DC, WC1, and WC2 to represent the dry specimens, wet specimens with a water content of 1.8%, and wet specimens with a water content of 3.6%.

2.2. Testing Methods. The servo-controlled RMT-150C system was used to conduct the uniaxial and triaxial compression experiments, as shown in Figure 3. A linear variable differential transformer (LVDT) was also used to measure the axial loading direction displacement for all compression tests, and its range and accuracy are 5 mm and 0.001 mm, respectively. The axial displacement loading rate was set to 0.002 mm/s. Four different confining pressure levels were selected, with values of 2, 4, 6, and 10 MPa.

Table 1: Industrial analysis parameters of the coal samples.

Calorific value cal. (g)	Coal moisture (%)	Ash (%)	Volatile (%)	Sulfur (%)
5800	2.26	24.94	39.13	1.43

Figure 1: Typical coal samples before water immersion.

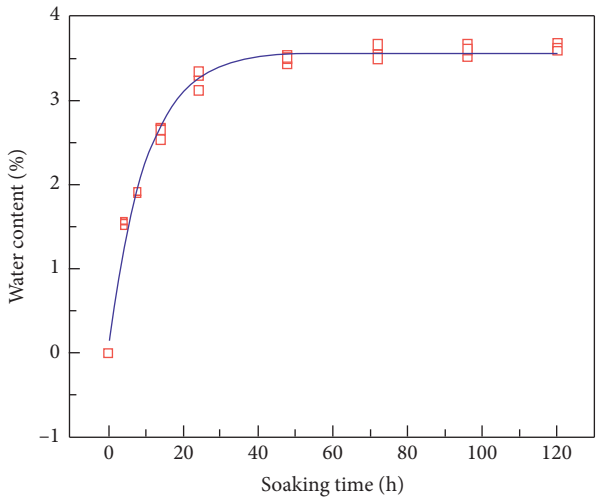

Figure 2: The relation between the water content and soaking time.

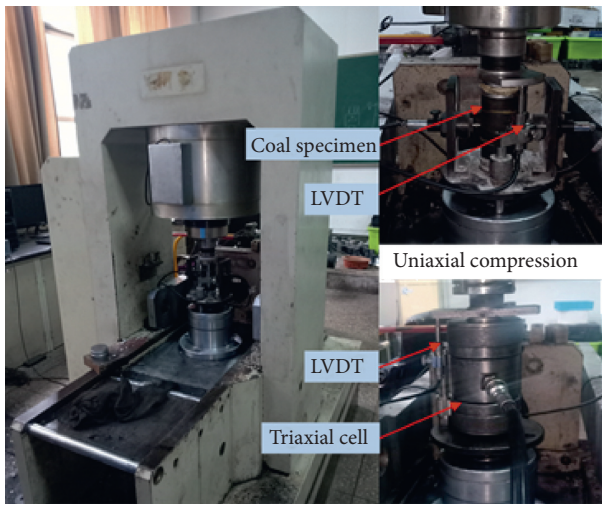

Figure 3: The RMT-150C experimental test system.

3. Uniaxial Compression Experimental Results

3.1. Stress-Strain Curves. The stress-strain curves and mechanical parameters of the coal specimens under uniaxial compression are presented in Figure 4 and Table 2, respectively. The slope of the straight line during the elastic stage was defined as the elastic modulus. Figure 4 shows that the stress-strain curves of coal specimens have four distinct stages: compaction, elasticity, yielding, and failure. In the compaction stage, a large deformation occurs, indicating that there are many initial fissures in the coal. The stress drops abruptly after it reaches the peak loading, showing a distinct brittle behavior.

The specimens exhibit several stress rises and drops during the yielding and failure stages; in particular, the deformation characteristics of wet specimens are very distinct. This phenomenon is in good agreement with the results of previous studies [29, 31]. This phenomenon contributes to the porous structure of the coal and the effect of water content.

3.2. Influence of Water Content on Uniaxial Compressive Strength. Figure 5 shows the relation between uniaxial compressive strength and water content. As seen from the figure, the uniaxial compressive strength decreases with increasing water content. When the coal samples have water contents of 1.8% and 3.6%, the uniaxial compressive strengths are reduced by 30.0% and 48.3%, respectively.

According to the suggestion by Hawkins and McConnell [19], the relation between uniaxial compressive strength and water content can be determined by the following equation:

$$\sigma_c(w) = a_0 e^{-bw} + a_1, \quad (2)$$

where σ_c is the uniaxial compressive strength, w is the water content, and a_0, a_1, and b are constants. Equation (2) shows that the uniaxial compressive strength can be determined at a water content of 0; the result is $a_0 + a_1$. Parameter b represents the reduction rate of strength with increasing water content. Based on the above analysis, the best-fit curve and the fitting equation are shown in Figure 5.

3.3. Influence of Water Content on Elastic Modulus. The relation between the elastic modulus and water content is presented in Figure 6. With increasing water content, the elastic modulus of coal specimens presented a significant reduction. The elastic moduli of the WC1 specimen (2.6 GPa) and the WC2 specimen (2.0 GPa) are 21.5% and 37.6% lower than that of the DC specimen (3.3 GPa). Compared with the uniaxial compressive strength reduction rate of 48.3%, the water content has less of a weakening influence on the elastic modulus. The relation between elastic modulus and water content is similar to the change law of the uniaxial compressive strength with water content.

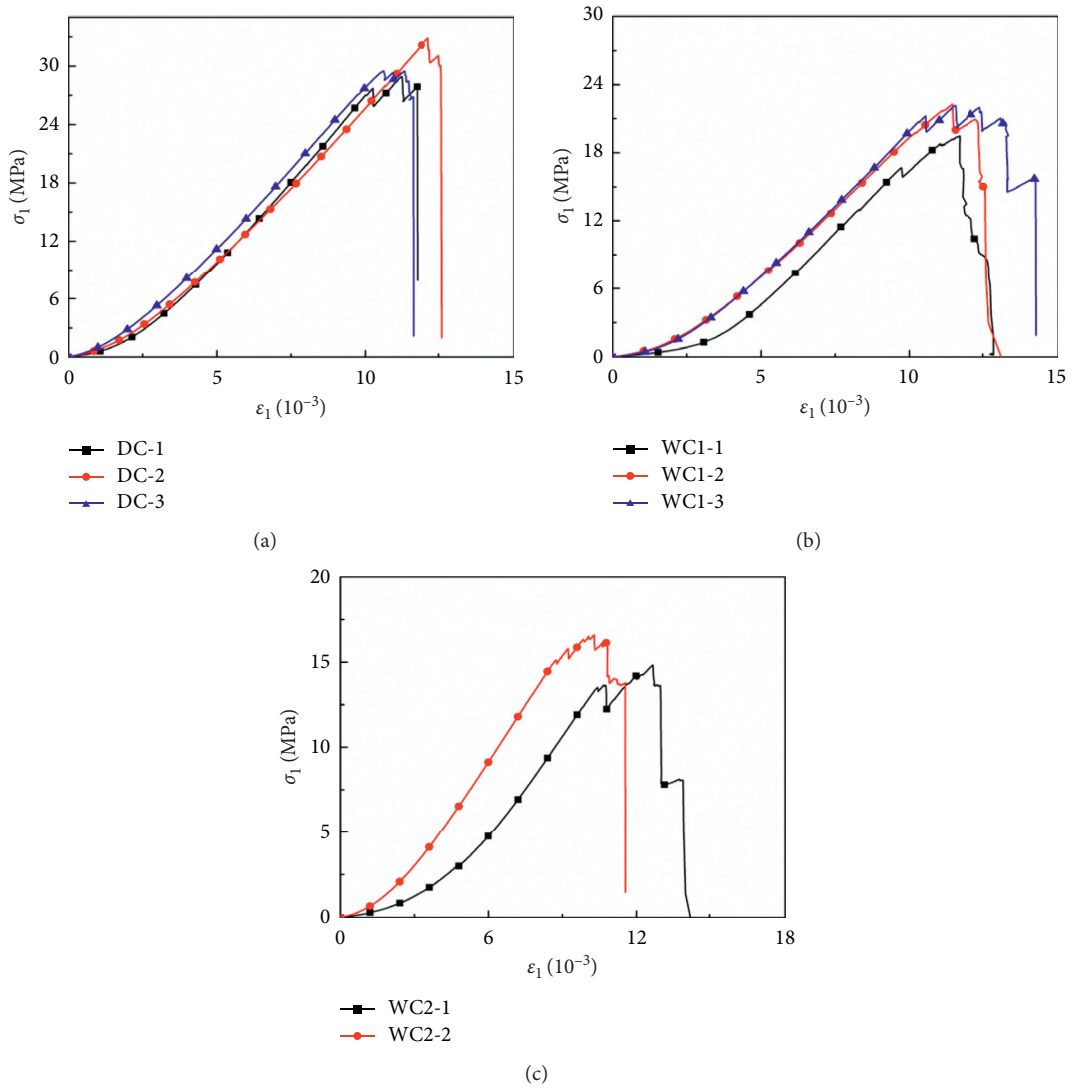

Figure 4: Stress-strain curves of the coal specimens under uniaxial compression: (a) DC group, (b) WC1 group, and (c) WC2 group.

Table 2: Mechanical parameters of specimens under uniaxial compression.

Specimen no.	Water content %		Uniaxial strength (MPa)	Elastic modulus (GPa)	Average strength loss rate %	Average elastic modulus loss rate %
	Designed	Real				
DC-1	0	0	28.9	3.4	0	0
DC-2		0	32.9	3.0		
DC-3		0	29.5	3.3		
Average		0	30.4	3.3		
WC1-1	1.80	1.78	19.5	2.6	30	21.5
WC1-2		1.69	22.3	2.5		
WC1-3		1.71	22.2	2.6		
Average		1.73	21.3	2.6		
WC2-1	3.60	3.51	14.8	1.9	48.3	37.6
WC2-2		3.62	16.6	2.2		
Average		3.57	15.7	2.0		

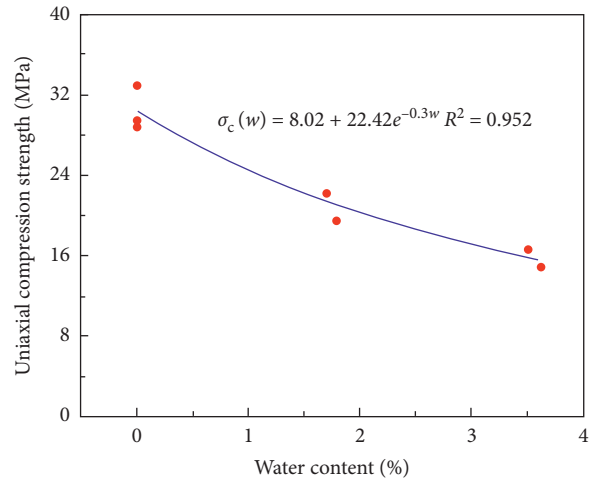

Figure 5: The relation between uniaxial compressive strength and water content.

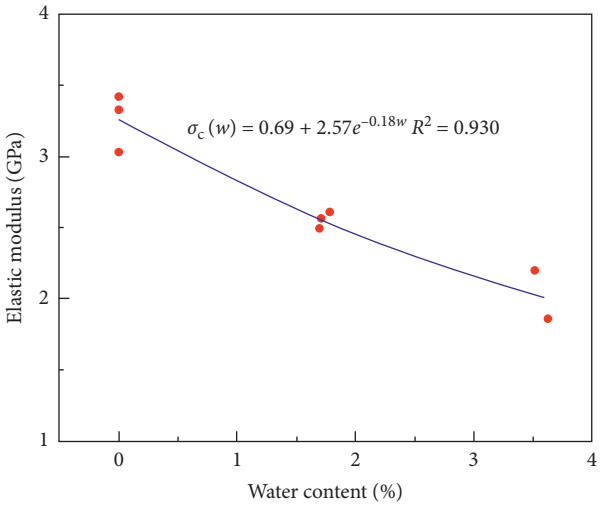

Figure 6: The relation between elastic modulus and water content.

The best-fit curve and the fitting equation are presented in Figure 6.

4. Triaxial Compression Experimental Results

4.1. Stress-Strain Curves. The stress-strain curves and mechanical parameters of coal specimens under triaxial compression are presented in Figure 7 and Table 3, respectively. A large deformation also occurs during the compaction stage, expanding the natural microfissure network in the specimen. With increasing confining pressure, the plastic deformation and bearing capacity of all the specimens increase, indicating that the confining pressure has an enhancement effect.

The deformation behavior of the dry specimens before peak loading is similar to that of the wet specimens, resulting in compaction, elasticity, and yielding stages, irrespective of water content. However, the water content has a great influence on the postfailure mechanical behavior. In the dry state, there was a clear stress-drop phenomenon after reaching the peak loading, showing a distinct brittle behavior, as shown in Figure 7(a). However, the stress of the wet specimen drops slowly during the postpeak stage, and it does not decrease to zero directly. The specimens still have a certain bearing capacity, as shown in Figures 7(b) and 7(c). This shows that the coal becomes "softer" with increasing water content. In this case, the bearing capacity of wet specimens mainly relied on the internal fissure friction of coal.

4.2. Strength Properties. Figure 8 shows the relations between the confining pressure and strength of the different groups of specimens under triaxial compression. It is found that the strengths of specimens at a confining pressure of 2 MPa are much greater than those of specimens under uniaxial compression. For example, the strengths of the DC specimen (61.8 MPa) and the WC1 specimen (48.7 MPa) at a confining pressure of 2 MPa are 203.3% and 219.4% greater than those of the DC specimen (30.4 MPa) and the WC1 specimen (22.2 MPa) under uniaxial compression. This is because of the difference in failure patterns [36, 37]. Under uniaxial compression, tensile and shear failures usually occur; however, the rock tested at a high confining pressure only presented a single shear failure.

As shown in Figure 8, the strengths of the three groups of specimens increased with increasing confining pressure, indicating that the confining pressure has a significant enhancement influence on the strength of coal. The confining pressure can contribute to the closure of cracks and fissures in the rock and prevent shear deformation between the fissures. Under the different confining pressures, the strengths of the dry specimens are obviously larger than those of the WC1 specimens and WC2 specimens, while the strengths of the WC2 specimens are the lowest compared to the strengths of the other two groups. This phenomenon indicates that the mechanical properties of coal can be affected by the water content.

The triaxial strengths of the WC2 specimens are lower than those of the WC1 specimens, indicating that the water content has a negative influence on the carrying capacity of coal. Compared with the uniaxial compressive strength reduction rate (48.3%), the confining pressure can inhibit the damage of water on the strength. As shown in Table 3, the strength loss rates under different confining pressures are lower than the values under uniaxial compression. For example, the strengths of the WC2 specimen and the WC1 specimen at the confining pressure of 10 MPa are 21.5% and 11.9% lower than those of the dry specimen.

4.3. Deformation Properties. Figure 9 shows the deformation properties of the different groups of specimens under triaxial compression. The elastic moduli of the specimens under uniaxial compression are lower than those of the specimens under triaxial compression. For example, the elastic modulus of the DC specimen (3.3 GPa) under uniaxial compression is 19.5% lower than that of the DC specimen (4.1 GPa) at a confining pressure of 2 MPa, as shown in Figure 9. This is also because microcrack propagation was inhibited by the confining pressure. The difference among

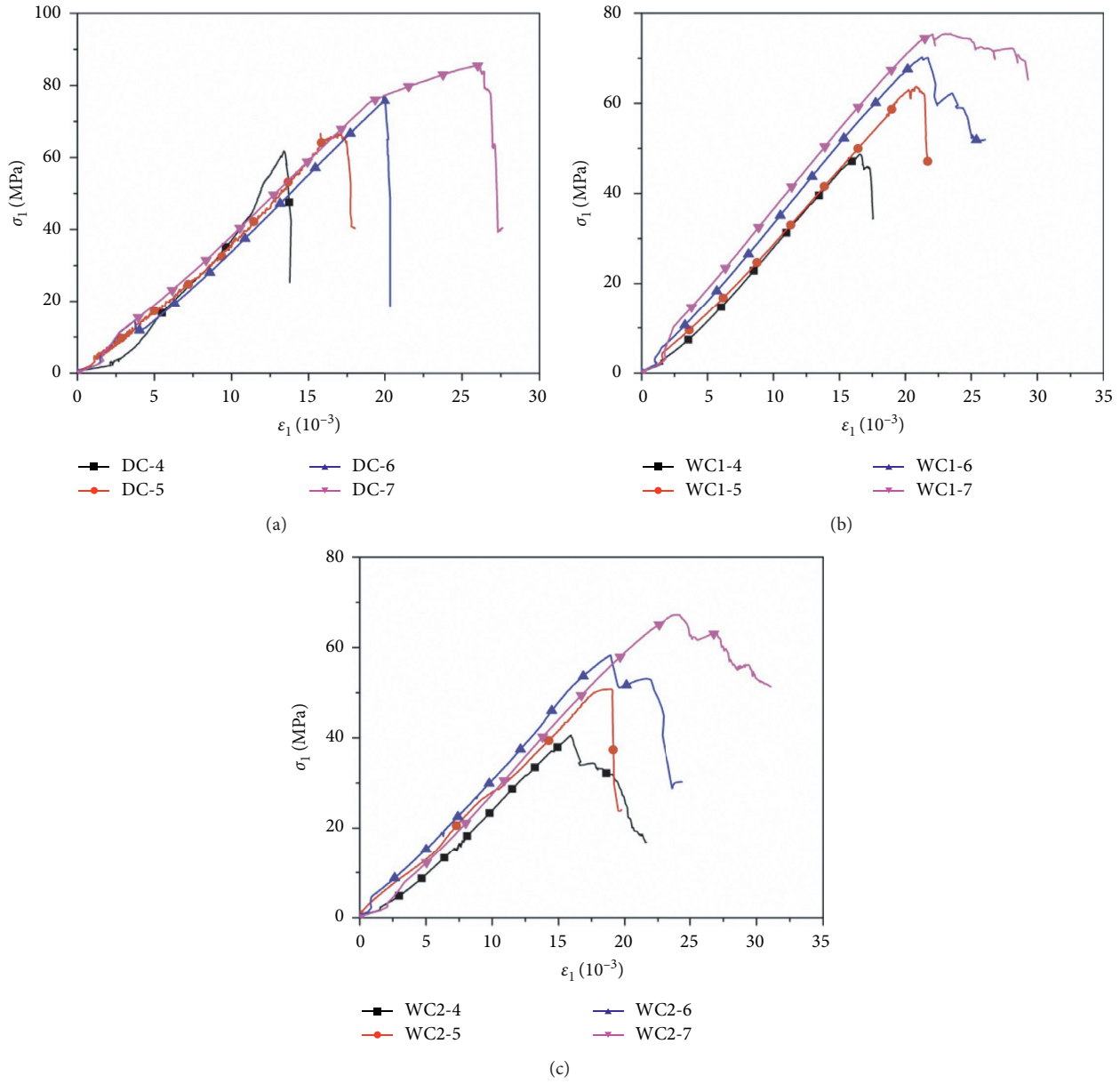

Figure 7: Stress-strain curves of the coal specimens under triaxial compression: (a) DC group, (b) WC1 group, and (c) WC2 group.

the elastic modulus results of the DC specimens tested under different confining pressures is small. This may be due to the heterogeneity of coal. In general, the elastic moduli of the WC1 and WC2 specimens increase with increasing confining pressure. The confining pressure has a positive effect on the elastic moduli of the wet specimens. It is noted that the elastic moduli of the WC1 and WC2 specimens are obviously lower than those of the DC groups. For example, the elastic modulus of the WC1 specimen (3.5 GPa) at a confining pressure of 6 MPa is 14.6%, which is higher than that of the DC specimen (4.1 GPa), as shown in Table 3. However, the elastic modulus of the WC2 specimen is lower than that of the WC1 specimen. In addition, the elastic modulus loss rates under different confining pressures are also lower than the values under uniaxial compression, as shown in Table 3.

4.4. Failure Patterns. Under uniaxial compression, the three groups of specimens exhibit mainly shear and tensile failures, as shown in Figure 10(a). For example, specimen DC-3 and specimen WC1-1 show distinct shear-tensile cracks. There are no obvious differences between the DC specimens and WC1 specimens. The WC2 specimens present serious fractures, and the coal was broken into small pieces.

Figure 10(b) shows the failure modes of the specimens under triaxial compression. Only one dry specimen formed a single main shear fracture face at a confining pressure of 10 MPa. Both shear and tensile fractures were observed on the faces of most specimens at different confining pressures; the failure patterns are similar to those under uniaxial compression. This phenomenon is in good agreement with the results of the studies by Diederichs et al. [36]. This means that there is a transition zone related to the tensile limit, and

Table 3: Mechanical parameters of specimens under triaxial compression.

Specimen no.	Water content (%)		Confining pressure (MPa)	Triaxial strength (MPa)	Elastic modulus (GPa)	Loss rate (%)	
	Designed	Real				Strength	Elastic modulus
DC -4	0	0	2	61.8	4.1	0	0
DC -5		0	4	66.7	3.8	0	0
DC -6		0	6	75.7	4.1	0	0
DC -7		0	10	85.6	4.0	0	0
WC1-4	1.80	1.69	2	48.7	3.4	21.2	17.1
WC1-5		1.78	4	63.8	3.2	4.3	15.8
WC1-6		1.77	6	70.3	3.5	7.1	14.6
WC1-7		1.82	10	75.4	3.6	11.9	10.0
WC2-4	3.60	3.57	2	40.6	2.8	34.3	31.7
WC2-5		3.56	4	50.8	2.8	23.8	26.3
WC2-6		3.52	6	58.3	3.1	23.0	24.4
WC2-7		3.62	10	67.2	3.3	21.5	17.5

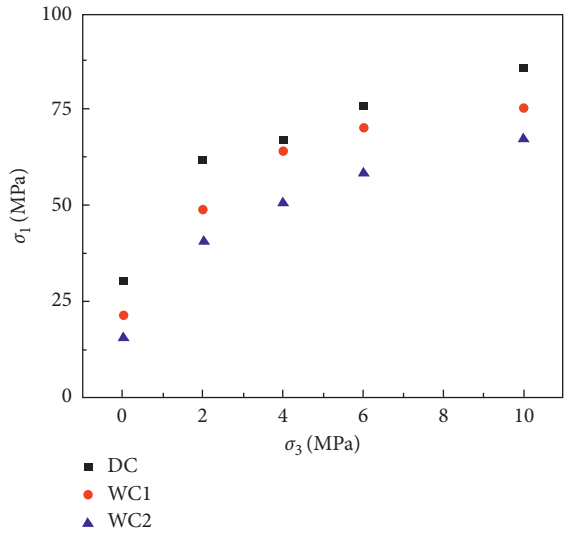

Figure 8: Relation between confining pressure and strength.

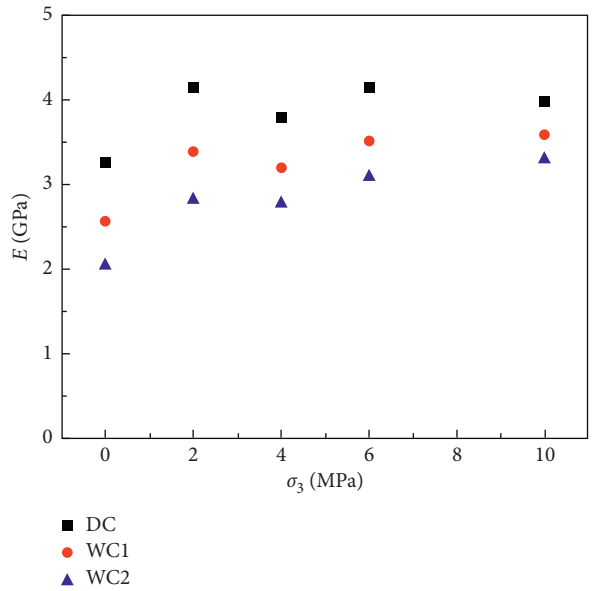

Figure 9: Relation between confining pressure and elastic modulus.

the rock specimens still form tensile cracks under conditions of low confining pressure. As shown in Figure 10(b), the sizes of the wet specimen fragments are obviously smaller than those of the dry specimen fragments, indicating that the failure modes can be affected by water content.

5. Discussion

5.1. Effect of Water Content on Microstructure. To intensively study the mechanism of water content on the weakening effect of coal, scanning electron microscopy was used to investigate the microscopic structure of coal with different water contents before the uniaxial and triaxial compression tests. The magnification used for the scanning electron microscopy work is 300 times.

As shown in Figure 11, the structure is clear and the surface is smooth when the coal in a dry state. When the water content is 1.8%, the surface of coal becomes rough and granular, indicating that the integrity of the coal sample worsens. With increasing water content, microcracks can clearly be found in the coal at a water content of 2.5%, and the length and width of the microcracks increase. The coal has poor integrity when the water content is 3.6%, and many microcracks are generated. The size of the microcracks increases with water content. In a local area, many acicular and laminated structures can be observed. As a whole, with increasing water content, the number and size of the microcracks in a coal sample will increase, and the structural integrity of the coal sample will deteriorate.

5.2. Effect of Water Content on Clay Minerals. According to the chemical components of coal, the percentage (39.15%) of AI_2O_3 is very high. This indicated that there are many clay minerals in the coal. Owing to their high superficial area and energy, clay minerals have a strong adsorption capacity. To interpret the effect of water on the clay minerals, Figure 12 shows the water absorption process of clay minerals. In the dry state, there are many cracks and clay minerals in the coal,

Figure 10: Failure modes of specimens: (a) the patterns under uniaxial compression and (b) the patterns under triaxial compression.

as shown in Figure 12(a). When the coal is immersed into the water environment, water flows inside and through the crack. Because clay minerals have strong hydrophilia, they will react with the water. The clay minerals will swell, resulting in the generation of a nonuniform swell stress in the coal, as shown in Figure 12(b). The swell stress will disintegrate mineral grains and smooth the irregular and serrated shapes around the grain contact periphery, resulting in the degradation of the mechanical performance of the coal, as shown in Figure 12(c).

5.3. Effect of Water Content on the Internal Friction Angle and Cohesive Force. To further study the weakening mechanism of water, the effects of water content on the internal friction angle and cohesive force were investigated. As shown in Figure 13, the strengths of the three groups increase linearly with increasing confining pressure. The relation between strength and confining pressure agrees with the Mohr–Coulomb strength criterion. In rock engineering, the Mohr–Coulomb strength criterion is widely used to study the mechanical parameters of rock [38]. The specific equation is as follows [38]:

$$\sigma_s = Q + K\sigma_3, \tag{3}$$

where Q and K are the strength parameters of the materials.

The relations between these strength parameters and the internal friction angle (φ) and cohesive force (c) are as follows:

$$\varphi = \arcsin\frac{K-1}{K+1}, \tag{4}$$

$$c = \frac{Q(1-\sin\varphi)}{2\cos\varphi}. \tag{5}$$

A linear regression was conducted, and the functional relationship is presented in Figure 13. According to (4) and (5), the internal friction angle and cohesive force of the three groups of specimens can be obtained. The internal friction angles of the DC, WC1, and WC2 specimens are 30.4°, 30.9°, and 31.9°, respectively. The cohesive forces of the DC, WC1, and WC2 specimens are 15.9, 13.5, and 10.1 MPa, respectively. It is found that the water content has almost no influence on the internal friction angle, while the water content has a significant effect on the cohesive force. The cohesive force of the WC2 specimen is 36.5% lower than that

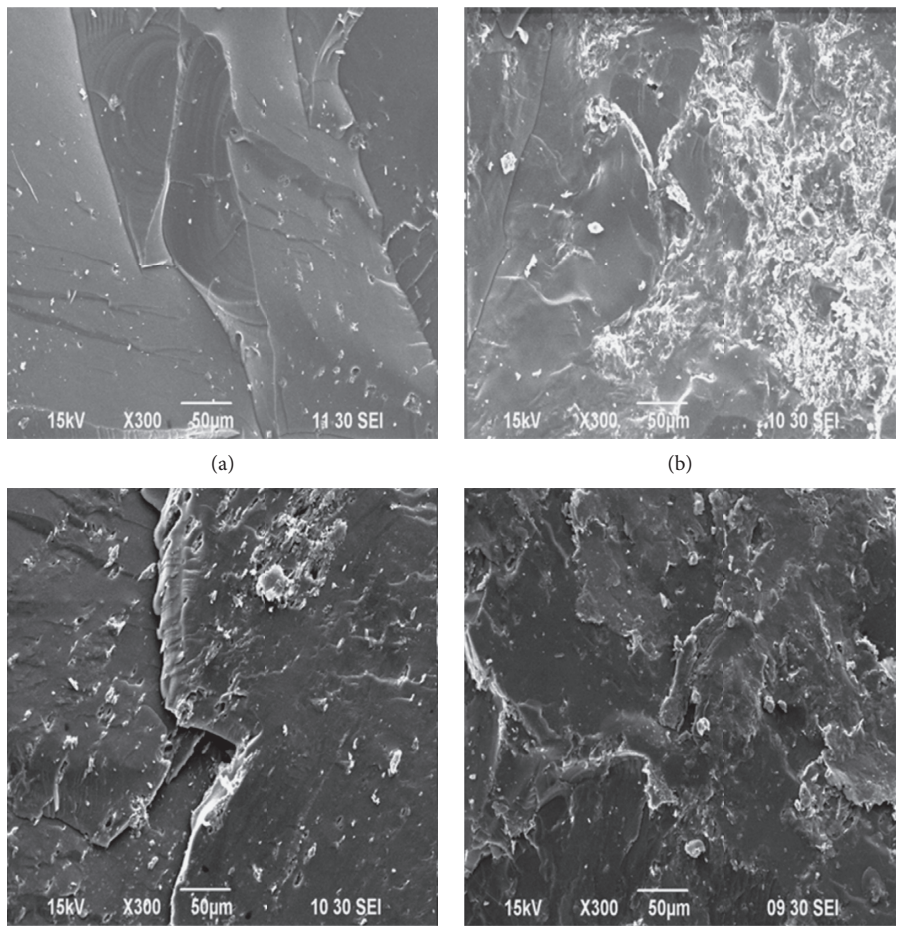

Figure 11: The microscopic structure of coal with different water contents. (a) Dry state. (b) Water content = 1.8%. (c) Water content = 2.5%. (d) Water content = 3.6%.

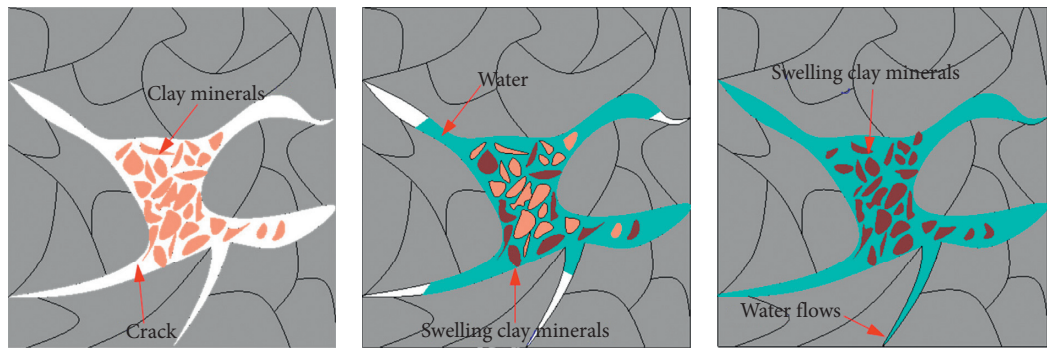

Figure 12: The water absorption process of clay minerals: (a) dry state, (b) water absorption state, and (c) saturation state.

of the WC1 specimen. This phenomenon also indicated that the internal friction angle is a material parameter, while the cohesive force is a structural parameter. Based on the above analysis, owing to the effect of water content on the microstructure and clay mineral properties, the structure becomes loose, and the cohesion between coal grains is

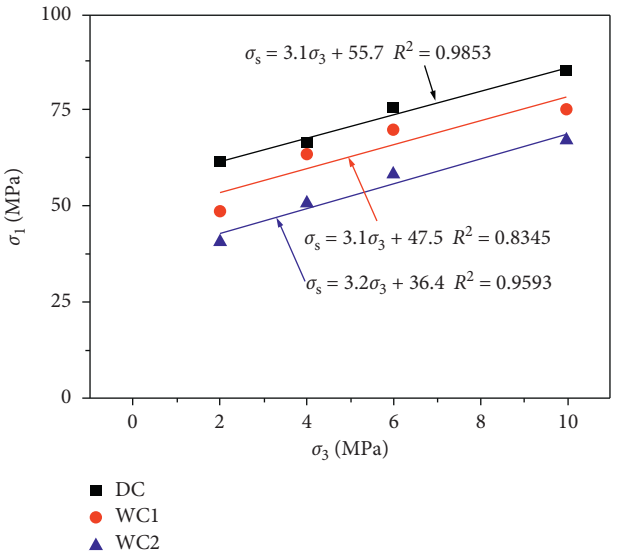

Figure 13: The functional relation between confining pressure and strength.

damaged. The microdamage in the coal contributes to the weakening of the cohesive force.

6. Conclusions

Coal bumps are common dynamic disasters in deep mines and are due to a sudden release of elastic energy in coal. This disaster involves the elastic energy in coal being greater than the dissipated energy, resulting in the ejection of coal. According to the test results in this study, the strengths and elastic moduli of wet specimens are clearly lower than those of dry specimens under different confining pressures. The water content has a significant influence on the postfailure mechanical behavior. As shown in Figure 7, the brittle characteristics weaken gradually with increasing water content, while the plastic characteristics of the coal are enhanced. This phenomenon shows that the elastic strain energy in coal decreases while the plastic deformation energy increases during the loading process. In other words, the risk of coal bumps decreases. In coal bump-prone mines, the aim of water injection is to increase the water content in the coal seam, reduce the strength, and enhance the plastic behavior of the coal, and thus the risk of coal bumps. This indicates that the results in this study can provide a good reference for preventing the occurrence of coal bumps during coal mining.

Based on this study, the main results are as follows:

(1) The uniaxial compressive strength and elastic modulus decrease with increasing water content, and both have an exponential relation with the water content. When the coal specimens reached the saturation state, the uniaxial compressive strength and elastic modulus decreased by 48.3% and 37.6% compared to those of the initial dry state, respectively.

(2) The water content has a great influence on the postfailure mechanical behavior. In the dry state, there is a clear stress-drop phenomenon after it reaches the peak loading, showing distinct brittle behavior. The stress in the wet specimen decreases slowly during the postpeak stage, exhibiting plastic deformation characteristics.

(3) The triaxial compressive strengths of the three groups of specimens increased with increasing confining pressure. The strengths and elastic moduli of the wet specimens are obviously lower than those of the dry specimens under different confining pressures. The confining pressure can inhibit the damaging effect of water on the mechanical properties of coal. The loss rates of the strength and elastic modulus decreased with increasing confining pressure.

(4) The scanning electron microscopy results show that the number and size of microcracks in the coal will increase with increasing water content, and the structural integrity of the coal will deteriorate. The hydration of clay minerals can lead to the reduction in the local cohesion of coal. The water content has almost no influence on the internal friction angle, while the cohesive force of the saturated specimens was 36.5% lower than that of dry specimens. Therefore, the internal friction angle is a material parameter, while the cohesive force is a structural parameter.

Data Availability

The data used to support the findings of this study are available from the corresponding author upon request.

Conflicts of Interest

The authors declare that they have no conflicts of interest.

References

[1] D. Song, E. Wang, Z. Liu, X. Liu, and R. Shen, "Numerical simulation of rock-burst relief and prevention by water-jet cutting," *International Journal of Rock Mechanics and Mining Sciences*, vol. 70, pp. 318–331, 2014.

[2] F. Feng, S. Chen, D. Li, S. Hu, W. Huang, and B. Li, "Analysis of fractures of a hard rock specimen via unloading of central hole with different sectional shapes," *Energy Science & Engineering*, vol. 7, no. 6, pp. 2265–2286, 2019.

[3] F. Feng, X. Li, J. Rostami, D. Peng, D. Li, and K. Du, "Numerical investigation of hard rock strength and fracturing under polyaxial compression based on mogi-coulomb failure criterion," *International Journal of Geomechanics*, vol. 19, no. 4, Article ID 04019005, 2019.

[4] Y. Jiang, Y. Zhao, H. Wang, and J. Zhu, "A review of mechanism and prevention technologies of coal bumps in China," *Journal of Rock Mechanics and Geotechnical Engineering*, vol. 9, no. 1, pp. 180–194, 2017.

[5] X. Chen and Y. Cheng, "Influence of the injected water on gas outburst disasters in coal mine," *Natural Hazards*, vol. 76, no. 2, pp. 1093–1109, 2015.

[6] B. Li, J. Liu, K. Bian et al., "Experimental study on the mechanical properties weakening mechanism of siltstone with

different water content," *Arabian Journal of Geosciences*, vol. 12, no. 21, p. 656, 2019.

[7] Q. Wu, L. Weng, Y. Zhao, B. Guo, and T. Luo, "On the tensile mechanical characteristics of fine-grained granite after heating/cooling treatments with different cooling rates," *Engineering Geology*, vol. 253, pp. 94–110, 2019.

[8] Z. Chen, X. Li, M. B. Dusseault, and L. Weng, "Effect of excavation stress condition on hydraulic fracture behaviour," *Engineering Fracture Mechanics*, vol. 226, Article ID 106871, 2020.

[9] E. M. Van Eeckhout and S. S. Peng, "The effect of humidity on the compliances of coal mine shales," *International Journal of Rock Mechanics and Mining Sciences & Geomechanics Abstracts*, vol. 12, no. 11, pp. 335–340, 1975.

[10] R. M. Iverson, "Landslide triggering by rain infiltration," *Water Resources Research*, vol. 36, no. 7, pp. 1897–1910, 2000.

[11] D. Ma, X. Cai, Q. Li, and H. Duan, "In-situ and numerical investigation of groundwater inrush hazard from grouted karst collapse pillar in longwall mining," *Water*, vol. 10, no. 9, p. 1187, 2018.

[12] H. Li, "Research on seepage properties and pore structure of the roof and floor strata in confined water-rich coal seams: taking the xiaojihan coal mine as an example," *Advances in Civil Engineering*, vol. 2018, Article ID 9483637, 8 pages, 2018.

[13] S. Ge, M. Liu, N. Lu, J. W. Godt, and G. Luo, "Did the zipingpu reservoir trigger the 2008 wenchuan earthquake," *Geophysical Research Letters*, vol. 36, no. 20, 2009.

[14] P. L. P. Wasantha and P. G. Ranjith, "Water-weakening behavior of Hawkesbury sandstone in brittle regime," *Engineering Geology*, vol. 178, pp. 91–101, 2014.

[15] I. Yilmaz, "Influence of water content on the strength and deformability of gypsum," *International Journal of Rock Mechanics and Mining Sciences*, vol. 47, no. 2, pp. 342–347, 2010.

[16] H.-w. Jing, Z.-y. Zhang, and G.-a. Xu, "Study of electromagnetic and acoustic emission in creep experiments of water-containing rock samples," *Journal of China University of Mining and Technology*, vol. 18, no. 1, pp. 42–45, 2008.

[17] B. Vasarhelyi, "Statistical analysis of the influence of water content on the strength of the miocene limestone," *Rock Mechanics and Rock Engineering*, vol. 38, no. 1, pp. 69–76, 2005.

[18] C. G. Dyke and L. Dobereiner, "Evaluating the strength and deformability of sandstones," *Quarterly Journal of Engineering Geology and Hydrogeology*, vol. 24, no. 1, pp. 123–134, 1991.

[19] A. B. Hawkins and B. J. Mcconnell, "Sensitivity of sandstone strength and deformability to changes in moisture content," *Quarterly Journal of Engineering Geology and Hydrogeology*, vol. 25, no. 2, pp. 115–130, 1992.

[20] K. Hashiba and K. Fukui, "Effect of water on the deformation and failure of rock in uniaxial tension," *Rock Mechanics and Rock Engineering*, vol. 48, no. 5, pp. 1751–1761, 2015.

[21] Z. Zhou, X. Cai, W. Cao, X. Li, and C. Xiong, "Influence of water content on mechanical properties of rock in both saturation and drying processes," *Rock Mechanics and Rock Engineering*, vol. 49, no. 8, pp. 3009–3025, 2016.

[22] D. Fan, X. Liu, Y. Tan et al., "Roof cutting parameters design for gob-side entry in deep coal mine: a case study," *Energies*, vol. 12, no. 10, pp. 1–25, 2019.

[23] J. Guo, G. Feng, T. Qi et al., "Dynamic mechanical behavior of dry and water saturated igneous rock with acoustic emission monitoring," *Shock and Vibration*, vol. 2018, Article ID 2348394, 14 pages, 2018.

[24] S. Wang, X. Li, J. Yao et al., "Experimental investigation of rock breakage by a conical pick and its application to non-explosive mechanized mining in deep hard rock," *International Journal of Rock Mechanics and Mining Sciences*, vol. 122, Article ID 104063, 2019.

[25] S. Wang, L. Huang, and X. Li, "Analysis of rockburst triggered by hard rock fragmentation using a conical pick under high uniaxial stress," *Tunnelling and Underground Space Technology*, vol. 96, Article ID 103195, 2020.

[26] S. Song, X. Liu, Y. Tan, D. Fan, Q. Ma, and H. Wang, "Study on failure modes and energy evolution of coal-rock combination under cyclic loading," *Shock and Vibration*, vol. 2020, Article ID 5731721, 16 pages, 2020.

[27] Z. Zhang, M. Deng, X. Wang, W. Yu, F. Zhang, and V. D. Dao, "Field and numerical investigations on the lower coal seam entry failure analysis under the remnant pillar," *Engineering Failure Analysis*, vol. 115, Article ID 104638, 2020.

[28] L. Weng, X. Li, A. Taheri, Q. Wu, and X. Xie, "Fracture evolution around a cavity in brittle rock under uniaxial compression and coupled static-dynamic loads," *Rock Mechanics and Rock Engineering*, vol. 51, no. 2, pp. 531–545, 2018.

[29] W. Wang, S. Zhang, H. Li, S. Gong, and Z. Liu, "Analysis of the dynamic impact mechanical characteristics of prestressed saturated fractured coal and rock," *Advances in Civil Engineering*, vol. 2019, Article ID 5125923, 10 pages, 2019.

[30] H. Gu, M. Tao, W. Cao, J. Zhou, and X. Li, "Dynamic fracture behaviour and evolution mechanism of soft coal with different porosities and water contents," *Theoretical and Applied Fracture Mechanics*, vol. 103, Article ID 102265, 2019.

[31] Q. Yao, X. Li, J. Zhou, M. Ju, Z. Chong, and B. Zhao, "Experimental study of strength characteristics of coal specimens after water intrusion," *Arabian Journal of Geosciences*, vol. 8, no. 9, pp. 6779–6789, 2015.

[32] Y. Liu, G. Yin, D. Zhang et al., "Directional permeability evolution in intact and fractured coal subjected to true-triaxial stresses under dry and water-saturated conditions," *International Journal of Rock Mechanics and Mining Sciences*, vol. 119, pp. 22–34, 2019.

[33] Q. Wu, X. Li, L. Weng, Q. Li, Y. Zhu, and R. Luo, "Experimental investigation of the dynamic response of prestressed rockbolt by using an SHPB-based rockbolt test system," *Tunnelling and Underground Space Technology*, vol. 93, Article ID 103088, 2019.

[34] Q. Wu, L. Chen, B. Shen, B. Dlamini, S. Li, and Y. Zhu, "Experimental investigation on rockbolt performance under the tension load," *Rock Mechanics and Rock Engineering*, vol. 52, no. 11, pp. 4605–4618, 2019.

[35] T. Szwedzicki, "International society for rock mechanics commission on testing methods: draft ISRM suggested methods for determining the indentation hardness index of rock materials," *International Journal of Rock Mechanics and Mining Sciences*, vol. 35, no. 6, pp. 831–835, 1998.

[36] M. S. Diederichs, P. K. Kaiser, and E. Eberhardt, "Damage initiation and propagation in hard rock during tunnelling and the influence of near-face stress rotation," *International Journal of Rock Mechanics and Mining Sciences*, vol. 41, no. 5, pp. 785–812, 2004.

[37] K. Du, C. Yang, R. Su, M. Tao, and S. Wang, "Failure properties of cubic granite, marble, and sandstone specimens under true triaxial stress," *International Journal of Rock Mechanics and Mining Sciences*, vol. 130, Article ID 104309, 2020.

[38] J. C. Jaeger, N. G. W. Cook, and R. W. Zimmerman, *Fundamentals of Rock Mechanics*, Blackwell Publishing Ltd., Oxford, UK, 4th edition, 2007.